

Parity-Violating Electron Scattering from ^4He and the Strange Electric Form Factor of the Nucleon

K. A. Aniol,¹ D. S. Armstrong,² T. Averett,² H. Benaoum,³ P. Y. Bertin,⁴ E. Burtin,⁵ J. Cahoon,⁶ G. D. Cates,⁷ C. C. Chang,⁸ Y.-C. Chao,⁹ J.-P. Chen,⁹ Seonho Choi,¹⁰ E. Chudakov,⁹ B. Craver,⁷ F. Cusanno,¹¹ P. Decowski,¹² D. Deepa,¹³ C. Ferdi,⁴ R. J. Feuerbach,⁹ J. M. Finn,² S. Frullani,¹¹ K. Fuoti,⁶ F. Garibaldi,¹¹ R. Gilman,^{14,9} A. Glamazdin,¹⁵ V. Gorbenko,¹⁵ J. M. Grames,⁹ J. Hansknecht,⁹ D. W. Higinbotham,⁹ R. Holmes,³ T. Holmstrom,² T. B. Humensky,¹⁶ H. Ibrahim,¹³ C. W. de Jager,⁹ X. Jiang,¹⁴ L. J. Kaufman,⁶ A. Kelleher,² A. Kolarkar,¹⁷ S. Kowalski,¹⁸ K. S. Kumar,⁶ D. Lambert,¹² P. LaViolette,⁶ J. LeRose,⁹ D. Lhuillier,⁵ N. Liyanage,⁷ D. J. Margaziotis,¹ M. Mazouz,¹⁹ K. McCormick,¹⁴ D. G. Meekins,⁹ Z.-E. Meziani,¹⁰ R. Michaels,⁹ B. Moffit,² P. Monaghan,¹⁸ C. Munoz-Camacho,⁵ S. Nanda,⁹ V. Nelyubin,^{7,20} D. Neyret,⁵ K. D. Paschke,⁶ M. Poelker,⁹ R. Pomatsalyuk,¹⁵ Y. Qiang,¹⁸ B. Reitz,⁹ J. Roche,⁹ A. Saha,⁹ J. Singh,⁷ R. Snyder,⁷ P. A. Souder,³ R. Subedi,²¹ R. Suleiman,¹⁸ V. Sulkosky,² W. A. Tobias,⁷ G. M. Urciuoli,¹¹ A. Vacheret,⁵ E. Voutier,¹⁹ K. Wang,⁷ R. Wilson,²² B. Wojtsekhowski,⁹ and X. Zheng²³

(HAPPEX Collaboration)

¹California State University, Los Angeles, Los Angeles, California 90032, USA

²College of William and Mary, Williamsburg, Virginia 23187, USA

³Syracuse University, Syracuse, New York 13244, USA

⁴Université Blaise Pascal/CNRS-IN2P3, F-63177 Aubière, France

⁵CEA Saclay, DAPNIA/SPHN, F-91191 Gif-sur-Yvette, France

⁶University of Massachusetts Amherst, Amherst, Massachusetts 01003, USA

⁷University of Virginia, Charlottesville, Virginia 22904, USA

⁸University of Maryland, College Park, Maryland 20742, USA

⁹Thomas Jefferson National Accelerator Facility, Newport News, Virginia 23606, USA

¹⁰Temple University, Philadelphia, Pennsylvania 19122, USA

¹¹INFN, Sezione Sanità, 00161 Roma, Italy

¹²Smith College, Northampton, Massachusetts 01063, USA

¹³Old Dominion University, Norfolk, Virginia 23508, USA

¹⁴Rutgers, The State University of New Jersey, Piscataway, New Jersey 08855, USA

¹⁵Kharkov Institute of Physics and Technology, Kharkov 310108, Ukraine

¹⁶University of Chicago, Chicago, Illinois 60637, USA

¹⁷University of Kentucky, Lexington, Kentucky 40506, USA

¹⁸Massachusetts Institute of Technology, Cambridge, Massachusetts 02139, USA

¹⁹Laboratoire de Physique Subatomique et de Cosmologie, 38026 Grenoble, France

²⁰St. Petersburg Nuclear Physics Institute of Russian Academy of Science, Gatchina, 188350, Russia

²¹Kent State University, Kent, Ohio 44242, USA

²²Harvard University, Cambridge, Massachusetts 02138, USA

²³Argonne National Laboratory, Argonne, Illinois, 60439, USA

(Received 8 June 2005; published 18 January 2006)

We have measured the parity-violating electroweak asymmetry in the elastic scattering of polarized electrons from ^4He at an average scattering angle $\langle\theta_{\text{lab}}\rangle = 5.7^\circ$ and a four-momentum transfer $Q^2 = 0.091 \text{ GeV}^2$. From these data, for the first time, the strange electric form factor of the nucleon G_E^s can be isolated. The measured asymmetry of $A_{\text{PV}} = (6.72 \pm 0.84_{\text{(stat)}} \pm 0.21_{\text{(syst)}}) \times 10^{-6}$ yields a value of $G_E^s = -0.038 \pm 0.042_{\text{(stat)}} \pm 0.010_{\text{(syst)}}$, consistent with zero.

DOI: 10.1103/PhysRevLett.96.022003

PACS numbers: 13.60.Fz, 11.30.Er, 14.20.Dh, 25.30.Bf

The complex structure of the nucleon goes well beyond its simplest description as a collection of three valence quarks. The sea of gluons and $q\bar{q}$ pairs that arise in quantum chromodynamics can play an important role, possibly even at long distance scales.

As the lightest explicitly nonvalence quark, the strange quark provides an attractive tool to probe the $q\bar{q}$ sea: there being no valence strange quarks, any strange quark con-

tributions must be effects of the sea. Thus a quark flavor decomposition of the various properties of the nucleon becomes of significant interest. In particular, a prominent open question is the strange quark contributions to the distributions of charge and magnetization.

The use of weak neutral current interactions as a key to providing a quark flavor separation of nucleon currents was first discussed nearly 20 years ago [1]. The Z^0 boson

interaction with the nucleon is described using form factors which are sensitive to a different linear combination of the light quark distributions than arise in the more familiar electromagnetic form factors. Thus, when combined with electromagnetic form factor data for the nucleon and the assumption of charge symmetry, neutral current measurements allow the disentangling of the contributions of the u , d , and s quarks [2–4].

Recently, experimental techniques have developed to the point of enabling measurements of sufficient precision to access strange quark effects. The strange quark contributions to the charge and magnetization of the nucleon are encoded in the strange electric and magnetic form factors, G_E^s and G_M^s , analogs of the usual Sachs form factors G_E and G_M .

The neutral current interaction can be accessed using parity-violating electron scattering, in which longitudinally polarized electrons are scattered from unpolarized targets. The cross section asymmetry $A_{PV} = (\sigma_R - \sigma_L)/(\sigma_R + \sigma_L)$ is formed, where $\sigma_{R(L)}$ is the cross section for right (left) handed electrons. This asymmetry, while typically tiny, of order a few parts per million (ppm), is caused by the interference of the weak and electromagnetic amplitudes, and so it isolates the neutral current form factors.

Recently, results of parity-violating electron scattering measurements on the proton at forward angles [5–8], and on the proton and deuteron at backward angles [9] have been reported. Each of these individual experiments is sensitive to different linear combinations of G_E^s , G_M^s , and the axial form factor G_A^{Zp} .

No individual experiment shows compelling evidence for nonzero strange quark effects. However, many available model calculations predicting significant strange form factors are allowed by the data. It is desirable to carry out complementary measurements that could help disentangle the contributions from the various form factors. In this Letter, we report on experiment E00114, the first measurement of A_{PV} for a ^4He target, which is sensitive to just one of the form factors: G_E^s , i.e., the strange quark charge distribution in the nucleon [2,10].

Elastic electron scattering from ^4He is an isoscalar $0^+ \rightarrow 0^+$ transition and therefore allows no contributions from magnetic or axial-vector currents. The parity-violating asymmetry at tree level is given by [3]

$$A_{PV}^{\text{He}} = \frac{G_F Q^2}{4\pi\alpha\sqrt{2}} \left(4\sin^2\theta_w + \frac{G_E^s}{G_E^{\gamma T=0}} \right), \quad (1)$$

where $G_E^{\gamma T=0} = (G_E^{\gamma p} + G_E^{\gamma n})/2$ is the isospin-zero electric form factor, which is adequately known from other experiments, and G_E^s is the electric strange quark form factor of the nucleon. G_F is the Fermi constant, α the fine structure constant, θ_w the weak mixing angle, and Q^2 the square of the 4-momentum transfer. The same one-body transition densities appear in the matrix elements of the weak and

electromagnetic operators. When the ratio comprising an asymmetry is formed, these transition densities cancel out, as long as two-body (meson-exchange) currents are negligible. Thus the nuclear many-body physics divides out and only the single nucleon form factors G_E^s and $G_E^{\gamma T=0}$ remain [3]. Nuclear model-dependence in A_{PV}^{He} due to isospin-mixing [11] and D -state admixtures [12] in the ^4He ground state is negligible, as are meson-exchange current contributions at the low Q^2 [10] of the present experiment.

The experiment was performed in Hall A at the Thomas Jefferson National Accelerator Facility. A $\sim 35 \mu\text{A}$ continuous-wave beam of longitudinally polarized 3.03 GeV electrons is incident on a 20 cm long cryogenic high-pressure ^4He gas target. Scattered electrons with $\theta_{\text{lab}} \sim 6^\circ$ are focused by two identical spectrometers onto total-absorption detectors. Only the electrons are detected from each scattering event; the second spectrometer merely doubles the accepted solid angle and provides some cancellation of systematic effects. The experimental approach largely parallels that of our previous measurement of parity-violating electron scattering on hydrogen at higher Q^2 , which is detailed in Ref. [13].

The spectrometer systems combine the Hall A high resolution spectrometers (HRS) [14] with new superconducting septum magnets [15]. The septa are necessary to deflect the 6° trajectories into the minimum accepted central angle for the HRS of 12.5° . Elastic trajectories are focused onto the detectors, spatially well separated from inelastic trajectories by the 12 m dispersion of the HRS. The elastic trajectories are intercepted by detectors composed of alternating layers of brass and quartz, oriented such that Cherenkov light generated by the electromagnetic shower is transported by the quartz to one end of the detector, to be collected by a photomultiplier tube (PMT).

The polarized electron beam originates from a GaAs photocathode excited by circularly polarized laser light. High polarization ($\sim 85\%$) of the extracted electron beam is achieved using an engineered superlattice of doped GaAs semiconductor layers [16]. The helicity of the beam is set every 33.3 ms locked to the 60 Hz ac power line frequency; we refer to each of these periods of constant helicity as a “window.” The helicity sequence consists of pairs of consecutive windows with opposite helicity; the helicity of the first window in each pair is determined by a pseudorandom number generator. The response of beam monitors and the electron detector PMTs is integrated over each window and then digitized by custom-built analog-to-digital converters.

The beam current is measured in the experimental hall with two independent rf cavities and the position of the beam is measured at multiple locations using rf stripline monitors. Typical intensity jitter at the 33 ms time scale is 600 ppm and position jitter on target is $20 \mu\text{m}$. Careful attention was given in design, component selection, and

configuration of the laser optics in the polarized source to avoid introducing a false asymmetry due to helicity-correlated changes in the electron beam properties. Averaged over the data taking, the helicity-correlated asymmetries in the electron beam were maintained below 0.075 ppm in intensity, 0.005 ppm in energy, 7 nm in position and 4 nrad in angle.

The data sample consists of roughly 3×10^6 pairs of windows, corresponding to a 60 h period. For each window, a distributed data acquisition system collects data from the polarized source electronics and the integrated response of the beam monitors and the detectors. Information on the helicity of the beam, delayed by 8 windows, is included in the data stream. To protect against false asymmetry from electronic pickup, no signal carries the helicity information away from the source region without this 8 window delay.

The only cuts applied to the data are to remove periods of either low beam current or rapidly changing current, or when a spectrometer magnet is off. No helicity-dependent cuts are applied.

The helicity-dependent asymmetry in the integrated detector response, normalized to the average beam intensity during each window, is computed for each pair of windows and then corrected for fluctuations in the beam trajectory to form the raw asymmetry A_{raw} . To first order, five correlated parameters describe the average trajectory of the beam during a window: energy, and horizontal and vertical positions and angles.

Two independent methods are used to calibrate the detector sensitivity to each beam parameter, and thus remove the beam-induced random and systematic effects from the raw detector-response asymmetry. The first uses a calibration subset of helicity windows, where each beam parameter is modulated periodically around its average value by an amount large compared to nominal beam fluctuations. The other method applies linear regression to the window pairs used in the physics analysis.

These techniques yield results which differ by a negligible amount compared to the final statistical error. Final results are obtained using the modulation technique. The cumulative correction for A_{raw} due to beam trajectory and energy asymmetry is -0.026 ppm.

The small beam intensity asymmetry of 0.075 ppm would induce a false asymmetry proportional to any alinearity in the detectors and beam current monitors. Using dedicated runs, the alinearity of the detector system is determined to be less than 1% and the relative alinearity between the beam monitors and the detectors is found to be less than 0.2%.

A half-wave ($\lambda/2$) plate is periodically inserted into the source laser optical path. This passively reverses the sign of the electron beam polarization, and hence the sign of A_{raw} , while leaving many possible systematic effects unchanged. Roughly equal statistics were accumulated with and without the $\lambda/2$ plate, thereby suppressing many systematic

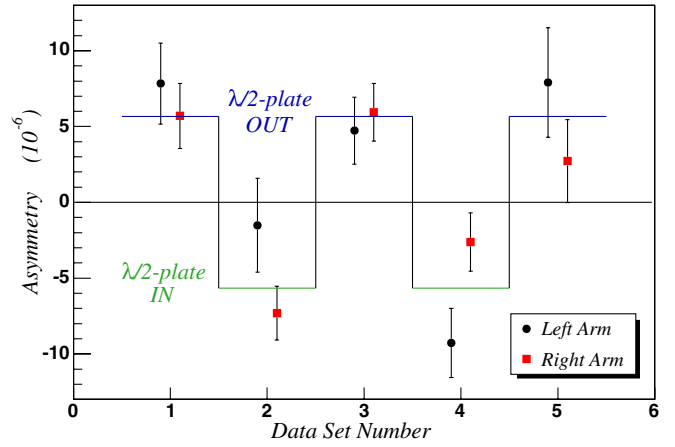


FIG. 1 (color online). Raw detector asymmetry A_{raw} for both spectrometers, broken down by data set. The step pattern represents the insertion/removal of a $\lambda/2$ plate at the beam source, which should flip the sign of the measured asymmetry.

effects. Figure 1 shows A_{raw} for all the data, grouped by periods of constant $\lambda/2$ -plate state.

The physics asymmetry $A_{\text{PV}}^{\text{He}}$ is formed from A_{raw} by correcting for beam polarization, backgrounds, and finite acceptance:

$$A_{\text{PV}}^{\text{He}} = \frac{K}{P_b} \frac{A_{\text{raw}} - P_b \sum_i A_i f_i}{1 - \sum_i f_i}, \quad (2)$$

where P_b is the beam polarization, f_i are background fractions and A_i the associated background asymmetries, and K accounts for the range of kinematic acceptance.

The beam polarization is measured in the experimental hall using a Compton polarimeter [17] which provides a continuous, noninvasive measurement simultaneous with data collection. Averaged over the run, the polarization is determined to be $P_b = (86.9 \pm 1.7)\%$. This result is consistent within error with results from dedicated runs to measure polarization using a Møller polarimeter [14].

Tracking chambers, part of the standard HRS detector package [14], are used to track individual events at the focal plane during dedicated, low-current runs in order to determine the average kinematics and to study backgrounds to the integrating measurement.

The total background is found to comprise $<3\%$ of the detector signal, of which inelastic scattering from ^4He is the largest component. The inelastic fraction is determined to be $(1.6 \pm 0.8)\%$ of the total detected flux by extrapolating the rise of the inelastic signal above the elastic radiative tail into the low-momentum edge of the detector—see Fig. 2. This contribution is dominated by quasielastic (QE) scattering.

The rescattering of electrons from various spectrometer apertures is another source of background. This is studied by varying the central spectrometer momentum in dedicated runs, and is determined to be $(0.6 \pm 0.6)\%$, domi-

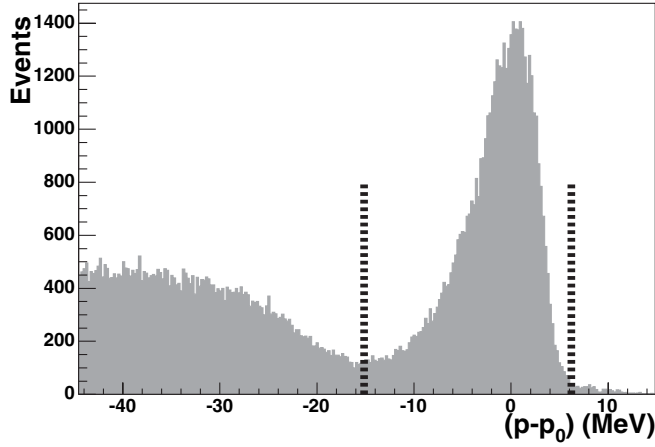


FIG. 2. Measured momentum difference from the central momentum (p_0) of one spectrometer, at the focal plane (filled histogram). Quasielastic scattering from ^4He dominates the data at low momenta. The vertical lines indicate the edges of the Cherenkov detector acceptance.

nated by QE scattering. Contributions from exposed iron pole tips in the dipole are negligible.

Background due to the aluminum windows of the cryogenic target is measured using an aluminum target with thickness matching the radiation length of the full target cell. The background is $(0.7 \pm 0.1)\%$ of the total detected rate; studies at low current to track individual counting events show that this contribution is dominated by QE scattering.

The corrections to the measured asymmetry for the QE scattering backgrounds discussed above are determined using the predicted [18] asymmetry of -1.6 ppm for both aluminum and ^4He , with a conservative 50% error assumed. The background corrections to A_{raw} are small and are listed in Table I.

The average Q^2 is determined to be $\langle Q^2 \rangle = (0.091 \pm 0.001) \text{ GeV}^2$ by dedicated low-current runs. Determination of Q^2 at this level requires precision measurement of the absolute scattering angle. Because of nuclear recoil, the scattering angle can be determined from the momentum difference between electrons elastically scattered from hydrogen and from a heavy nucleus. A water-cell target provided a target containing hydrogen and the heavier oxygen nuclei. The scattering angle into pinholes

of a sieve collimator at the entrance of each spectrometer is measured using this method to a precision of 0.3%.

Results from the two spectrometers agree within the statistical errors and are averaged together. After all corrections, the asymmetry is found to be $A_{\text{PV}}^{\text{He}} = 6.72 \pm 0.84 \pm 0.21$ ppm, where the first error is statistical and the second systematic. Individual contributions to the systematic error are detailed in Table II.

The theoretical value for the asymmetry from Eq. (1), under the assumption that $G_E^s = 0$, including the vector electroweak radiative corrections (0.9%) [3], is $A_{\text{PV}}^{\text{He}}|_{G_E^s=0} = 7.483$ ppm. The effect of purely electromagnetic radiative corrections is negligible due to the spin independence of soft photon emission and the small momentum acceptance of the detectors. For the electromagnetic form factor $G_E^{\gamma T=0}$ we have used a recent phenomenological fit to the world data at low Q^2 [19], with a total uncertainty of 2.6%. Comparing $A_{\text{PV}}^{\text{He}}|_{G_E^s=0}$ to our measured $A_{\text{PV}}^{\text{He}}$ we extract the value of the strange electric form factor $G_E^s = -0.038 \pm 0.042 \pm 0.010$, which is consistent with zero. The first uncertainty is statistical and the second is systematic, including those due to radiative corrections and electromagnetic form factors.

There have been numerous attempts to calculate strange form factors using a host of models and theoretical approaches (see Ref. [4] and references therein). Available calculations do not even agree on the sign of G_E^s , and predicted values range from -0.08 to $+0.08$. The present result disfavors models with large positive values, e.g., Refs. [20,21].

We have also made a measurement of A_{PV} from the proton at a very similar Q^2 , which is reported in an accompanying paper [22]. The combination of the two measurements, as well as with previous measurements at the same Q^2 [7,9] allows access to both G_E^s and G_M^s separately [22]. A new run of this experiment took place recently which is expected to improve the statistical precision by a factor of 3, along with a modest reduction in the systematic error.

In summary, we have made the first measurement of the parity-violating asymmetry in elastic electron scattering from ^4He , which is uniquely sensitive to the strange electric form factor G_E^s . The result obtained is consistent with zero, and constrains models of the strangeness in the nucleon.

TABLE I. Corrections to A_{raw} .

	Correction (ppm)
Target windows	0.058 ± 0.012
QE ^4He	0.129 ± 0.070
Rescattering	0.049 ± 0.050
Beam Asyms.	-0.026 ± 0.102
Alinearity	0.000 ± 0.077

TABLE II. Systematic uncertainties.

Normalization Factors	
Polarization P_b	0.869 ± 0.017
Acceptance K	1.000 ± 0.001
Q^2 Scale	1.000 ± 0.010

We thank the superb staff of Jefferson Lab for their contributions to the success of this work. This work was supported by DOE Contract No. DE-AC05-84ER40150, Modification No. M175 under which the Southeastern Universities Research Association (SURA) operates the Thomas Jefferson National Accelerator Facility, and by the Department of Energy, the National Science Foundation, the Istituto Nazionale di Fisica Nucleare (Italy), the Commissariat à l'Énergie Atomique (France), and the Centre National de Recherche Scientifique (France).

-
- [1] D. B. Kaplan and A. Manohar, Nucl. Phys. **B310**, 527 (1988); R. D. McKeown, Phys. Lett. B **219**, 140 (1989).
 - [2] D. H. Beck, Phys. Rev. D **39**, 3248 (1989).
 - [3] M. J. Musolf *et al.*, Phys. Rep. **239**, 1 (1994).
 - [4] K. S. Kumar and P. A. Souder, Prog. Part. Nucl. Phys. **45**, S333 (2000); D. H. Beck and R. D. McKeown, Annu. Rev. Nucl. Part. Sci. **51**, 189 (2001); D. H. Beck and B. R. Holstein, Int. J. Mod. Phys. E **10**, 1 (2001).
 - [5] K. A. Aniol *et al.*, Phys. Rev. Lett. **82**, 1096 (1999); K. A. Aniol *et al.*, Phys. Lett. B **509**, 211 (2001).
 - [6] F. E. Maas *et al.*, Phys. Rev. Lett. **93**, 022002 (2004).
 - [7] F. E. Maas *et al.*, Phys. Rev. Lett. **94**, 152001 (2005).
 - [8] D. S. Armstrong *et al.* (G0 Collaboration), Phys. Rev. Lett. **95**, 092001 (2005).
 - [9] D. T. Spayde *et al.*, Phys. Lett. B **583**, 79 (2004); T. M. Ito *et al.*, Phys. Rev. Lett. **92**, 102003 (2004).
 - [10] M. J. Musolf, R. Schiavilla, and T. W. Donnelly, Phys. Rev. C **50**, 2173 (1994).
 - [11] S. Ramavataram, E. Hadjimichael, and T. W. Donnelly, Phys. Rev. C **50**, 1175 (1994).
 - [12] M. J. Musolf and T. W. Donnelly, Phys. Lett. B **318**, 263 (1993).
 - [13] K. A. Aniol *et al.*, Phys. Rev. C **69**, 065501 (2004).
 - [14] J. Alcorn *et al.*, Nucl. Instrum. Methods Phys. Res., Sect. A **522**, 294 (2004).
 - [15] P. Brindza *et al.*, IEEE Trans. Appl. Supercond. **11**, 1594 (2001).
 - [16] T. Maruyama *et al.*, physics/0412099.
 - [17] S. Escoffier *et al.*, Nucl. Instrum. Methods Phys. Res., Sect. A **551**, 563 (2005).
 - [18] M. J. Musolf and T. W. Donnelly, Nucl. Phys. **A546**, 509 (1992); **A550**, 564(E) (1992).
 - [19] J. Friedrich and Th. Walcher, Eur. Phys. J. A **17**, 607 (2003); we adopt their fit version 1.
 - [20] H. Weigel *et al.*, Phys. Lett. B **353**, 20 (1995).
 - [21] A. Silva, H. C. Kim, and K. Goeke, Phys. Rev. D **65**, 014016 (2002); **66**, 039902(E) (2002).
 - [22] K. A. Aniol *et al.*, nucl-ex/0506011.